POAC'13
Espoo, Finland

Proceedings of the 22nd International Conference on
Port and Ocean Engineering under Arctic Conditions
June 9-13, 2013
Espoo, Finland

EXTREME KEEL DRAFTS IN THE FRAM STRAIT 2006-2011

Ole-Christian Ekeberg[1,2], Knut Høyland[1,3], Edmond Hansen[4]
[1]Norwegian University of Science and Technology (NTNU), Trondheim, NORWAY
[2] Det Norske Veritas, Bærum, NORWAY
[3]Sustainable Arctic Marine and Coastal Technology (SAMCoT), Centre for Research-based Innovation (CRI), Norwegian University of Science and Technology, Trondheim, NORWAY
[4] Norwegian Polar Institute, Tromsø, NORWAY

ABSTRACT

Knowledge about extreme keel drafts is needed for appropriate design of offshore installations in ice ridge infested waters. Ice drafts were measured with upward looking sonar by the Norwegian Polar Institute in the western part of the Fram Strait along 79°N in the period 2006 to 2011. This is where the Transpolar Drift exits the Arctic Ocean, and the ice consists of a mixture of first-year and old ice originating from most parts of the Arctic Ocean. In total, 8 year-long deployments at 4 locations were analyzed. A generalized Pareto distribution was fitted to all ridges deeper than 17 m. This only amounts to a small fraction of all the ridges, but follows the methodology common for the calculation of extremes. All ridges deeper than 25 m were investigated prior to the analysis to ensure that no icebergs or other misidentified features were included. In total, 5 identified ridges were removed. The deepest ridge observed in the period was 35 m deep and 5 more ridges were deeper than 30 m in these 8 deployment seasons. Since the shape parameter in the generalized Pareto Distribution was close to zero the distribution could be simplified into an exponential distribution. Assuming an exponential distribution gave an estimated 100-year return value in the range 37 to 41 m.

INTRODUCTION

Ice ridges are often the governing design action for both platforms and pipelines in areas with a dynamic ice cover. It is therefore of great importance to know how deep ridge keels could be in the area in question. This is usually estimated through an extreme value analysis. Due to the limited amount of available ice draft data, only a few extreme ridge keel depth analyses are published (Melling and Riedel, 1995; Melling and Riedel, 1996; Pilkington and Wright, 1991; Ross et al., 2012; Wadhams, 1983; Wadhams, 2012).

Data used for the extreme value analysis above are all based on upward looking sonar (ULS). A ULS measures the ice draft above the sonar and the final product is a time series if the ULS is moored to the seabed or a spatial series if the ULS is mounted to a submarine. The moored ULS can be supplemented by an ADCP which measures the ice drift speed and allows a conversion into a spatial series (Melling et al., 1995). A time series is sufficient for an analysis of extreme drafts at a specific location.

While Wadhams (1983) uses spatial ice draft data from a submarine mounted ULS, Ross et al. (2012) estimate return values based on data from a moored ULS. The latter data are better suited for the estimation of extremes at a point since spatial draft data must be complemented by ice drift speed to get a point estimate. Wadhams (1983, 2012) has found that the ice ridge keel draft can be approximated by an exponential distribution. Ross et al. (2012) obtain this indirectly as they apply the Weibull distribution but find that the shape parameter is close that which corresponds to exponential distribution.

A minimum draft is used to filter out ridges which are too shallow to include in the extreme value analysis. While Ross et al. (2012) follow common methodology in extreme value analysis and apply high thresholds ($h_k > 15$ m), Wadhams (1983, 2012) fits the exponential distribution to all ridges deeper than 5 m. We use the generalized Pareto distribution with a range of thresholds to investigate the stability of the results. The shape parameter (ξ) was close to zero for most tested settings. This means that the generalized Pareto distribution could be simplified to exponential distribution. In combination with a threshold value of 17 m the exponential distribution seems to provide the most reasonable estimate of the 100-year return value which then is in the range 37-41 m.

METHOD

Ice draft data were collected by the Norwegian Polar Institute (NPI) using an Ice Profile Sonar (described by Melling et al., 1995) in the period 2006-2011 in the Fram Strait (Hansen et al., 2013). The moorings with the sonars were placed at 4 different locations at the edge of the Greenland continental shelf (Table 1). In total, 8 measurement seasons (lasting from September to September) were used. No data exist from 2007/2008 due to very heavy ice conditions in August/September 2007, which hindered the annual retrieval and re-deployment of the moorings.

The Ice Profile Sonar (IPS) measures the ice draft every 2 seconds and prior to the ridge identification the data were smoothed with a running average filter with a window size of 10 seconds (5 points). The smoothing was done to minimize effects from erroneous draft readings which could create artificial gaps which the ridge identification criterion uses as an identifier for a new ridge. Ice ridges were identified using the Rayleigh criterion (Wadhams and Horne, 1980) with a threshold value of 2.5 m and a minimum draft of 10 m. The Rayleigh criterion defines an individual ice ridge when the ice thickness on each side of a local maxima descends at least halfway toward the threshold value. The extreme value analysis only considers the draft (or more specifically the maximum draft) of the ice ridges.

All ridges deeper than 25 m were manually inspected. In total there were 47 ridges deeper than 25 m of which 5 ridges were removed. That included the deepest feature which was measured to be 38.2 m and probably was an iceberg. This iceberg was actually deeper than 38.2 m but since this was too close to the IPS it was recorded as out of range and only given an error code.

Table 1. The location of each mooring and which measurement seasons that were used.

Location (coordinate)	2006/2007	2008/2009	2009/2010	2010/2011
F11 (78°50'N,3° W)				X
F12 (78°50'N,4°W)			X	X
F13 (78°50'N,5°W)	X	X		
F14 (78°50'N,6°30’W)	X	X	X	

Extreme value model - generalized Pareto family

A generalized Pareto distribution (GPD) model was used for the extreme value modeling. The GPD facilitates the use of more than block maxima which a traditional General Extreme Value (GEV) model uses. If $X_1, X_2, ...$ are independent and identically distributed random variables the generalized Pareto family approximates (1) and is described by (2) where ξ is the shape parameter and σ the scale parameter, $F(X)$ is the common distribution function, $H(y)$ is the distribution function of $(X - u)$ and u is the threshold value (Coles, 2001). In the special case where the shape parameter $\xi = \rightarrow 0$ this becomes the exponential distribution with parameter $1/\tilde{\sigma}$.

$$\Pr(X > u + y | X > u) = \frac{1 - F(u + y)}{1 - F(u)}, y > 0 \quad (1)$$

$$H(y) = 1 - \left(1 + \xi \cdot \frac{y}{\tilde{\sigma}}\right)^{-1/\xi} \quad (2)$$

Defined on $(y: y > 0$ and $\left(1 + \xi \cdot \frac{y}{\tilde{\sigma}}\right) > 0)$, where

$$\tilde{\sigma} = \sigma + \xi(u - \mu) \quad (3)$$

and σ corresponds to the shape parameter from the corresponding GEV model.

The corresponding parameter estimates $(\hat{\xi}, \hat{\sigma})$ are found by maximum likelihood estimation. Maximum likelihood finds the model which the observations are most likely to have been drawn from. For a given probability distribution$f(x)$, with parameters θ (here ξ and σ), the most likely parameter estimates are found by maximizing (4). Since its logarithm also maximizes at the same parameter estimate the log-likelihood is used for simplicity (5).

$$L(\theta) = \prod_{i=1}^{n} f(x_i; \theta) \quad (4)$$

$$l(\theta) = \log\big(L(\theta)\big) = \sum_{i=1}^{n} \log(f(x_i; \theta)) \quad (5)$$

Return levels for a given shape and scale could be calculated from (6) except when $\xi = 0$ then (7) is applied. ζ_u is the fraction of ridges above the given threshold u, while N is the return period in years and *npy* is the number of observations per year.

$$x_m = u + \frac{\sigma}{\xi}\left[(N \cdot npy \cdot \zeta_u)^{\xi} - 1\right] \quad (6)$$

$$x_m = u + \sigma \cdot \log(N \cdot npy \cdot \zeta_u) \quad (7)$$

Confidence intervals of both return periods and parameter estimates could be approximated assuming normality of the parameter estimates but as Coles (2001) shows, better estimates could be found from the log-likelihood estimate. The maximum log-likelihood estimate (MLE) defines the upper limit in the parameter space while the lower limit is defined as the MLE subtracting half the corresponding quantile from the chi-square distribution with one degree of freedom (χ_1^2). Correspondingly, the high and low confidence limits of each parameter are found on this maximum likelihood surface.

RESULTS

Shape parameter

The shape parameter (ξ) was zero except for a slight increase above a threshold of 20 m (Figure 1). It equaled 0 well within the confidence interval of 95 % for all thresholds. This suggested that an exponential distribution can be used for the calculation of extremes. The scale parameter $\tilde{\sigma}$ is then the only calculated parameter and hence it governs the return value estimate (7). An exponential distribution (EXP) resulted in higher extremes for the low thresholds and significantly narrower confidence intervals compared to the generalized Pareto Distribution (GP) (Figure 3).

The data were divided into one eastern and one western data series. By varying the threshold value and by excluding particular seasons in each of the two datasets the sensitivity of the shape parameter was tested. When the 2006/2007 season was left out from the westernmost series, the shape parameter was about -0.1 (~2006 in Figure 2). This was not observed in the easternmost series, although the fraction of 2006/2007 ridges was similar. There were significantly more ridges observed in 2006/2007 than in any of the subsequent seasons (Figure 4). An analysis only considering the deepest ridge per hour also showed stability in the shape estimate (Figure 2).

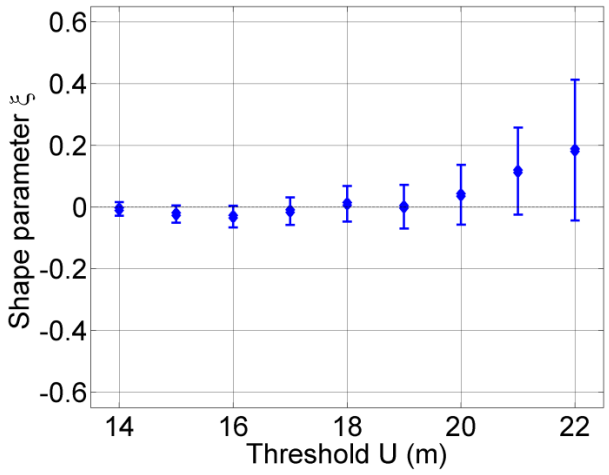

Figure 1. The estimated shape parameter as a function of threshold (u) with 95 % confidence intervals.

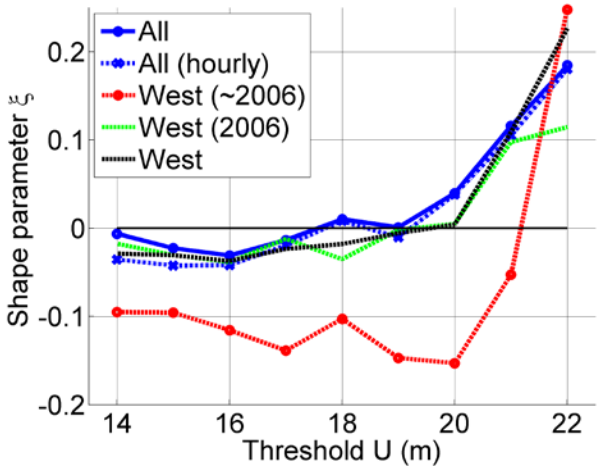

Figure 2. Shape parameter estimates for the westernmost series, including all 4 seasons, leaving out (~) 2006/2007 and including only 2006/2007.

Return level

Return level estimates are consistent for thresholds between 14 m and 22 m when the uncertainty in the estimates is taken into account (Figure 3). All the data, observed for 4 seasons at two parallel locations, gave a 100-year return value between 37 m and 41 m (Figure 3).

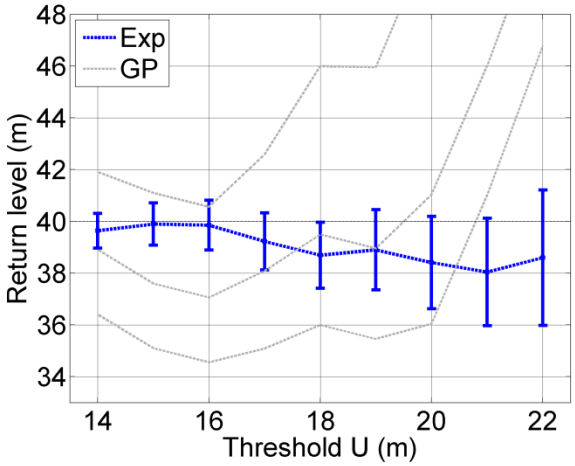

Figure 3. The 100-year return level for varying threshold assuming 8 years of observations The 95 % confidence interval is included in the bars. Results for the generalized Pareto distribution are shown in gray including its 95 % confidence bounds.

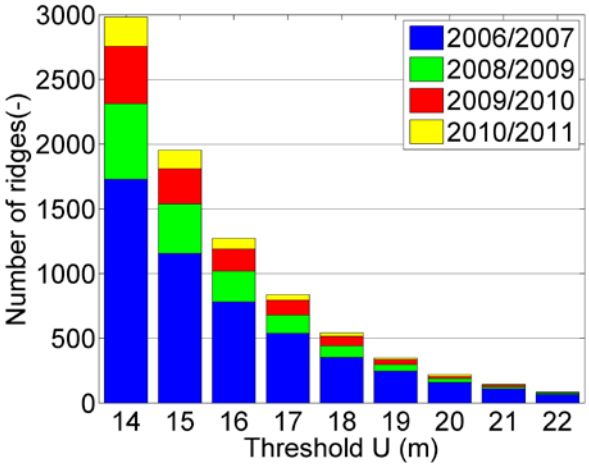

Figure 4. Number of ridges per season above the given threshold.

Inter-seasonal variation

An extreme value analysis using all the available data (red line), fits the observed data well (blue circles) with a slight underestimation of the three deepest ridges (Figure 5). There was large variation between each individual measurement-season (gray crosses). The western probability distribution was more consistent than the eastern with respect to the difference that was apparent from including/excluding the 2006/2007 season (Figure 6).

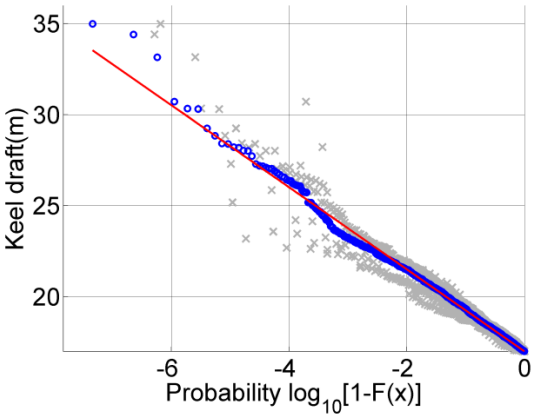

Figure 5. A probability plot of all individual seasons (gray x) and the entire dataset (blue o). The red line is the estimate assuming $\xi = 0$ based on all data and threshold of 17 m.

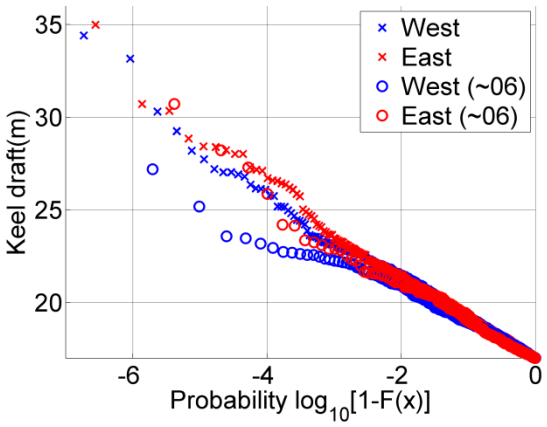

Figure 6. A probability plot based on each series in Table 1 and threshold of 17 m. For each location the 2006/2007 season is included (x) or excluded (o).

Threshold value

The return level with a variable return period was calculated for both an exponential distribution ($\xi = 0$) and a Pareto distribution (Figure 7). The estimated return level was more consistent for various thresholds when applying the exponential distribution. The 100-year return level varied between 38 and 41 depending on the method and threshold value which was similar to that observed in Figure 3. Since the thresholds 14 m and 17 m both have shape parameter estimates close to zero (Figure 1) the estimates between the two distributions were similar. A threshold of 20 m resulted in larger deviation which is related to the positive but moderate shape estimate (ξ~0.05). When the confidence intervals were included, the differences between the methods were revealed (Figure 8). An exponential distribution will predict on a narrower confidence band than the Pareto distribution. This difference in confidence interval is discussed in Coles (2001) who argues that the Pareto distribution estimate better reflects the uncertainty connected with extrapolating model results.

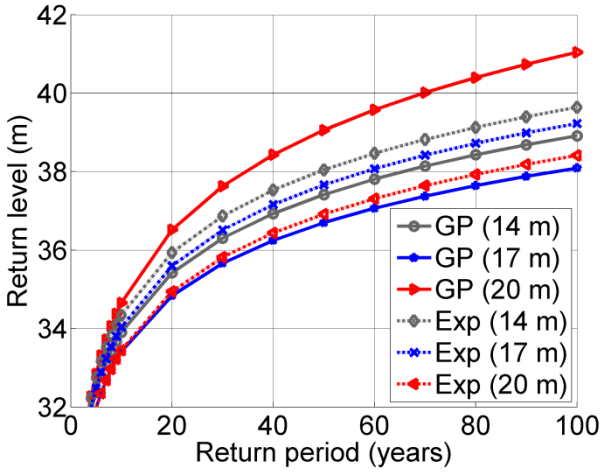

Figure 7. The return value for variable return period, threshold and method.

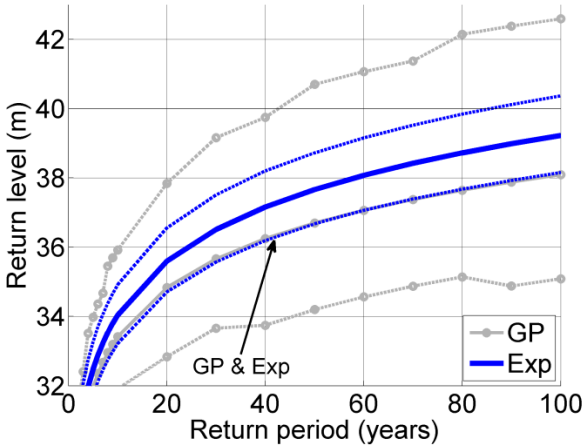

Figure 8. Return level vs. return period for the exponential distribution (Exp) and the generalized Pareto distribution (GP). Both with 95 % confidence intervals and a threshold of 17 m.

Model configuration

A threshold of 17 m was chosen to be the most representative for this extreme value analysis and the model fitted the observations well (Figure 9).

An increasing threshold *u* reduces observations for the inference but should decrease the bias. Stability was present both in the shape and the return level for the increasing threshold (Figure 1 and Figure 3). This gave confidence that while a lower *u* increased the bias it decreased the variance. A threshold of about 17 m seemed to balance the variation and bias well. Both an exponential distribution model and a generalized Pareto model were able to reproduce most observations but slightly underestimated the draft of the deepest ridges (Figure 9).

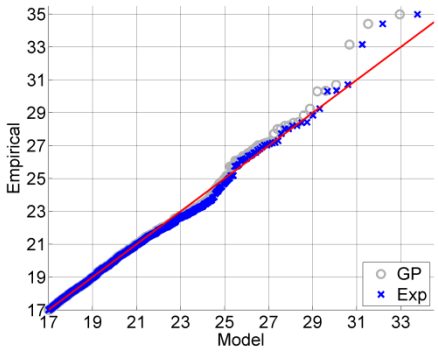

Figure 9. A quantile plot of the estimate from both models using a threshold of 17 m. The red reference line is where the model predicts the same as the observed.

DISCUSSION

The present extreme value analyses provide an estimate of how deep an ice ridge could be in North East Greenland. This is an area which is of increasing interest to the oil and gas industry and such an extreme value analysis could provide valuable input to design of structures to be used in this area. Ice that floats out the Fram Strait also origins from most of the Arctic Ocean. Although how a very deep ridge deteriorates over time is unknown, the extremes observed in the Fram Strait indicate the extremes in the Arctic Ocean.

Independent and identically distributed observations

We expect that the dependency between observations of very deep ridges is reduced with the time and distance to the event which formed them. In the Fram Strait, when and where the ridges are formed is unknown and could vary from locally formed ridges to ridges formed several years ago in far away locations.

Unfortunately this time series is limited in time which disallows the use of a block maxima model like the General Extreme Value model. Instead the inference was based on the generalized Pareto Model which uses more of the observations than only a block maxima. We assumed that ridges deeper than 14 m were approximately independent. An increase in threshold is expected to increase the chance that the observations are independent. Thus when the results proved similar regardless of the threshold the assumption about independency is supported. This is further supported from the division into two series and by only considering the hourly maxima which all produced similar results.

An exception was the dependency on 2006/2007 in the westernmost series which, whether included or not, had a major impact on the estimated shape parameter (Figure 2) and thus the return value. This deviation could indicate that the data are non-stationary. Non-stationarity is also in line with recent changes in the ice draft distribution (Hansen et al., 2013) and the reduction in old ice (Kwok et al., 2009). However stationarity is a very complex property to study (Lins, 2012) and the present time series is too short for this kind of study.

It is clear that 2006/2007 was a year of more frequent ridges with a higher probability of encountering a large ice ridge. But while the probability of exceedance for the western data

depends on whether or not the 2006/2007 data are included, this effect was not present in the easternmost series. The probability of exceedance for each individual measurement season suggested that there are major differences between years (Figure 5), which do not strictly justify assumptions about identical distributions.

Relation to other studies

Previous studies have used both the exponential distribution (Wadhams, 1983 and 2012) and the Weibull distribution (Ross et al., 2012) to estimate extreme keel drafts. The generalized Pareto distribution is, as already shown, equal to the exponential distribution when $\xi = 0$. The same applies for the Weibull distribution which reduces to the exponential distribution when its shape parameter is 1.

In the present study the shape parameter was close to zero and justified the use of the exponential distribution. Ross et al. (2012) found that the Weibull-shape parameter for various thresholds was approximately 1. This suggests that both the present study and Ross et al. (2012) predicted similar results to those found by Wadhams (2012). To illustrate the potential similarities between these three approaches the Weibull-, generalized Pareto and the exponentialdistributions were fitted to all samples above a threshold of 17 m (Figure 10). All distributions were approximated with the log-likelihood method (5). Since the parameter estimate in the Weibull is close to 1 and the shape parameter in the generalized Pareto distribution was close to 0 they predict almost identical 100 year return values (circles in Figure 10).

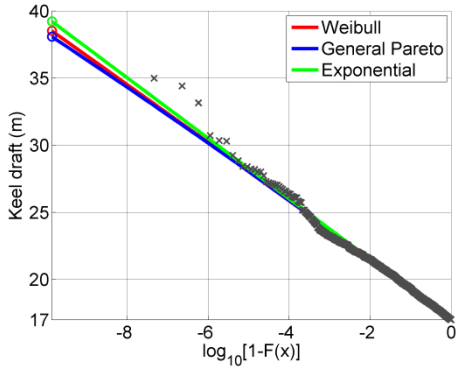

Figure 10. A comparison of the extreme value estimates obtained by using the Weibull-, the generalized Pareto- or the exponentialdistributions with a threshold of 17 m. The crosses are observations while the circles are the corresponding 100 year return value.

Ross et al. (2012) predicted return values for the Fram Strait based on based the 2 measurement seasons in 2008/2009 which were included in this analysis. They found that the 100-year return value was about 33±4 m which is somewhat low compared to our results. Since we have 3 observations above 33 m in 8 measurement seasons the estimate of Ross et al. (2012) is probably too low. An estimate in the upper range of their suggestion is more in line with the present findings (Figure 8). Wadhams on the other hand found that the return value in the Beaufort is in the range 30-35 m which is very close to the estimate by Ross et al. who found this to be 32±2 m.

Ice ridge keel action

The ice ridge draft is highly relevant for the calculation of ridge keel action on structures. An important point is to distinguish between extreme features such as the draft of an ice ridge and the extreme responses used for design. The action from an ice ridge keel on a structure is a combination of the keel geometry, velocity, and strength of the ridge keel. Hence an extremely deep ridge keel does not necessarily result in the largest design action or the largest responses.

Another aspect of load calculation is which part of the ice ridge that should be included. Figure 11 shows an ice ridge which is deepened by what could be a level ice piece. Should the maximum depth of the ridge be set according to what is expected to be contributing mostly to the load? And in this case should we then reduce the ridge draft here from 25.5 m to 20.5 m? In the present study we chose to leave this as it is. To automate such a criterion involves subjective criteria and could be difficult to implement. Another reason to leave this within the study follows from ISO19906 (2010). This suggests that the confinement in the ridge keel increases from zero at the very deepest point up to the consolidated layer. By removing bottom features it is likely that the keel bottom has higher consolidation than expected which leads to an underestimation of the load from the ridge keel.

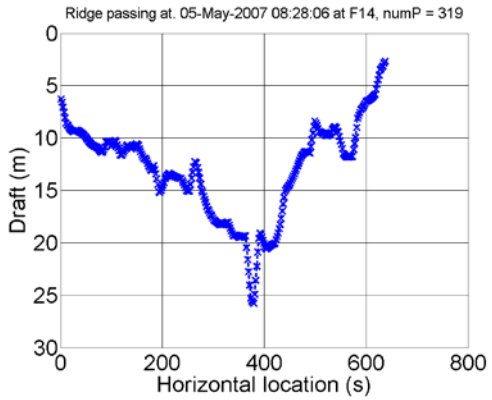

Figure 11. The maximum draft of this particular ice ridge might be deepened by a piece of ice. This makes the maximum draft of the ridge 5 m deeper.

CONCLUSION

An extreme value analysis of extreme keel drafts has been conducted using a generalized Pareto distribution. Data were obtained from upward looking sonars placed along 79°N at edge of the Greenland continental shelf between 2006 and 2011. In total, 8 measurement seasons of upward looking sonar data were used. The deepest feature in this period was 35 m deep and a total of 6 ridges were deeper than 30 m.

The generalized Pareto distribution was simplified to the exponential distribution since its shape parameter ξ was close to zero. An exponential distribution in combination with a threshold of 17 m gave a 100-year return value in the range 37-41 m. This is somewhat higher than previous studies of extreme keel drafts in the same area and also higher than corresponding estimates for the Beaufort Sea.

ACKNOWLEDGEMENTS

Ole-Christian Ekeberg acknowledges fruitful discussions with his colleague Erik Løkken Walter at Det Norske Veritas. The authors also wish to acknowledge the support from the Research Council of Norway through PetroRisk and the Centre for Research-based Innovation SAMCoT and the support from all SAMCoT partners.

REFERENCES

Coles, S., 2001. An Introduction to Statistical Modeling of Extreme Values. Springer Series in Statistics. Springer.

Hansen, E., Gerland, S., Granskog, M., Pavlova, O., Renner, A., Haapala, J. and Løyning, T.B., 2013. Thinning of Arctic sea ice in Fram Strait: 1990-2011. (submitted to Journal of Geophysical Research January 2012).

ISO19906, 2010. Petroleum and natural gas industries - Arctic offshore structures, ISO19906, Geneva, Switzerland.

Kwok, R., Cunningham, G.F., Wensnahan, M., Rigor, I., Zwally, H.J. and Yi, D., 2009. Thinning and volume loss of the Arctic Ocean sea ice cover: 2003–2008. Journal of Geophysical Research: Oceans, 114(C7): n/a-n/a.

Lins, H.F., 2012. A Note on Stationarity and Nonstationarity. WMO.

Melling, H., Johnston, P.H. and Riedel, D.A., 1995. Measurements of the Underside Topography of Sea Ice by Moored Subsea Sonar. Journal of Atmospheric and Oceanic Technology, 12(3): 589-602.

Melling, H. and Riedel, D.A., 1995. The underside topography of sea ice over the continental shelf of the Beaufort Sea in the winter of 1990. J. Geophys. Res., 100(C7): 13641-13653.

Melling, H. and Riedel, D.A., 1996. Development of seasonal pack ice in the Beaufort Sea during the winter of 1991-1992: A view from below. J. Geophys. Res., 101(C5): 11975-11991.

Pilkington, R. and Wright, B.D., 1991. Beaufort Sea ice thickness measurements from an acoustic under ice, upward looking ice keel profiler, First International Offshore and Polar Engineering Conference. The International Society of Offshore and Polar Engineers Edinbourough, United Kingdom, pp. 456-461.

Ross, E., Fissel, D.B., Marko, J.R. and Reitsma, A., 2012. An improved method for extremal value analysis of arcitc sea ice thickness derived from upward looking sonar ice data, Arctic Technology Conference. OTC, Houston, Texas, pp. OTC 23811.

Wadhams, P., 1983. The prediction of extreme keel depths from sea ice profiles. Cold Regions Science and Technology, 6(3): 257-266.

Wadhams, P., 2012. New predictions of extreme keel depths and scour frequencies for the Beaufort Sea using ice thickness statistics. Cold Regions Science and Technology, 76–77(0): 77-82.

Wadhams, P. and Horne, R.J., 1980. An analysis of ice profiles obtained by submarine sonar in the Beaufort Sea. Journal of Glaciology, 25(93): 401-423.